

On-line Monitoring and Parameter Estimation of a Microbial Fuel Cell Operated with Intermittent Connection of the External Resistor

Javier Coronado*, Boris Tartakovsky**, Michel Perrier*

*Département de Génie Chimique, École Polytechnique Montréal, C.P.6079 Succ.,
Centre-Ville Montréal, QC, Canada H3C 3A (e-mail: michel.perrier@polymtl.ca).

**National Research Council of Canada, 6100 Royalmount Ave.,
Montréal, QC, Canada H4P 2R2 (e-mail: Boris.Tartakovsky@cnrc-nrc.gc.ca)

Abstract: This study describes on-line monitoring and parameter estimation during Microbial Fuel Cell operation with a pulse-width modulated connection of the external resistor (R-PWM mode) at low and high frequencies. Analysis of the output voltage profiles acquired during R-PWM tests showed the presence of slow and fast dynamic components, which can be described by an equivalent circuit model suitable for process monitoring and control applications. To demonstrate the proposed monitoring and parameter estimation procedure, the MFC was operated at several influent concentrations of acetate (carbon source) and an on-line parameter estimation procedure was used for estimating internal resistance and internal capacitance. Furthermore, these parameters were re-estimated at the end of each test yielding similar results. The proposed on-line procedure can be used for real-time process optimization.

Keywords: Microbial Fuel Cell; Real-time monitoring; parameter estimation; Internal resistance.

1. INTRODUCTION

Electricity production from organic wastes in Microbial Fuel Cells (MFCs) offers a new and sustainable technological solution capable of converting otherwise energy-consuming wastewater treatment into an energy-neutral, and potentially an energy-producing process.

Recent advances in MFC design and materials helped to improve volumetric power output by several orders of magnitude (Logan 2010). Yet, to be competitive with the existing wastewater treatment technologies, power densities should be further improved. While researchers continue to make progress by improving the electrode materials and MFC design (Logan and Rabaey 2012; Lovley 2008; Rozendal et al. 2008), the need for a real-time maximum power point tracking system becomes apparent.

MFC power output might be maximized by matching the external impedance with the MFC internal impedance. Unlike in more traditional power sources, the internal impedance of a MFC strongly depends on a variety of operating conditions including wastewater composition and organic matter concentration (Martin et al. 2010). Therefore, an on-line monitoring and parameter estimation procedure might be required for performance optimization. Based on the principle of power supply by means of commuting (switching) circuits, hysteresis controllers have been implemented to track the Maximum Power Point (MPP) of a MFC (Park and Ren 2011). Also, a perturbation-observation algorithm was used to optimize MFC electrical load in real time showing a considerably improved power output (Pinto et al. 2011). A simple heuristic approach was implemented to

automatically control the electrical load attached to the MFC (Premier et al. 2011).

Our previous work demonstrated that by operating an MFC with intermittent connection/disconnection of the electrical load (external resistance), the MFC power output could be improved (Grondin et al. 2012). The study presented below demonstrates that a simple equivalent circuit model can be used for on-line monitoring and parameter estimation of a MFC operated with intermittent connection/disconnection of the external resistance at a sufficiently high switching frequency, equivalent to a pulse-width modulated connection of the external resistance (R-PWM mode of operation).

2. EXPERIMENTAL

2.1 MFC design and Operation

A membrane-less air-cathode MFC was constructed using nylon plates as described elsewhere (Grondin et al. 2012). The anode was 10 mm thick carbon felts measuring 10 cm × 5 cm (SGL Canada, Kitchener, ON, Canada) and the cathode was 10 cm x 5 cm manganese - based catalyzed carbon E4 air cathodes (Electric Fuel Ltd, Bet Shemesh, Israel). The electrodes were separated by a nylon cloth. The MFC had an anodic compartment volume of 50 mL and contained two carbon felt anodes and two cathodes (one on each side connected by a wire). The MFC was maintained at 25°C and was continuously fed with sodium acetate and trace metal solutions. An influent acetate concentration of 900 mg L⁻¹ (normal influent concentration) or 1800 mg L⁻¹ (high influent concentration) and a hydraulic retention time of 6-7 h were

typically maintained. A detailed description of MFC design, stock solution composition, and operating conditions can be found elsewhere (Grondin et al. 2012).

2.2 External Resistance Connection

Pulse-width modulated connection of the external resistor (R_{ext}) to MFC terminals was achieved by adding an electronic switch (IRF540, International Rectifier, El Segundo, CA, USA) to the external electrical circuit (Fig. 1B). The switch was computer-controlled using a Labjack U3-LV data acquisition board (LabJack Corp., Lakewood, CO, USA). The data acquisition board was also used to record MFC voltage at a maximum rate of 22,500 scans/s.

As shown in Fig. 1, the data acquisition board measured MFC output voltage (U_{MFC}) and voltage at the switch (U_{sw}). Voltage over the resistive load (U_L) was calculated as the difference between U_{MFC} and U_{sw} ($U_{Load} = U_{MFC} - U_{sw}$). Electric current was calculated as $I = U_{Load} / R_{Load}$ by applying Ohm's law over the external load resistance (R_{Load}).

For calculation purposes, the switching device was considered as an ideal switch in series with a resistance R_{sw} to represent power losses in the switch. R_{sw} value was estimated by dividing the voltage over the switch by the current. In the following discussion, R_{ext} denotes the sum of the external load connected to the circuit and the switch resistance ($R_{ext} = R_{Load} + R_{sw}$).

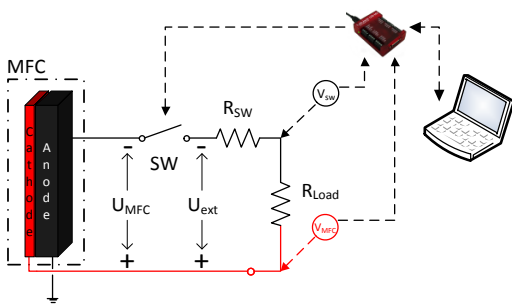


Fig. 1. Electrical circuit of the MFC.

2.2 Numerical Methods

Computer simulations were carried out using the equivalent circuit model and model solutions described below. Parameter estimation was carried out using `fmincon` function of Matlab R2010a (Mathworks, Natick, MA, USA). In the parameter estimation procedure the root mean square error between the model outputs and measured values of U_{MFC} was minimized using data of five on/off cycles. At a R-PWM frequency of 0.1 Hz this corresponded to 637 data points. At a frequency of 100 Hz, 1000 data points were used to estimate model parameters. The on-line parameter estimation procedure is described below.

3. RESULTS AND DISCUSSION

Analysis of MFC output voltage at high and low frequency of R_{ext} connection/disconnection suggests that the observed dynamics can be described by a simple equivalent circuit model (Randles model) previously used for modeling batteries and simulating a MFC power management system (Durr et al. 2006; Yang et al. 2012).

The equivalent circuit model (ECM) consisted of two internal resistors and one internal capacitor. Figure 2 shows the model diagram, where U_{oc} corresponds to MFC's open circuit voltage (ideal voltage), C represents the MFC capacitance, R_1 accounts for the MFC's ohmic losses, and R_2 represents the resistive component accounting for both the activation and concentration losses (Yang et al. 2012).

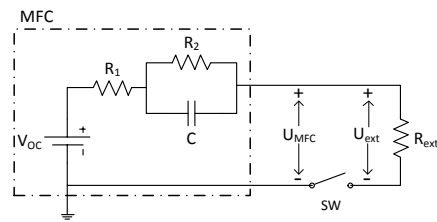


Fig. 2. MFC Equivalent Circuit Model.

The following first order differential equation describes voltage dynamics :

$$\frac{dU_c(t)}{dt} = \frac{U_{oc}}{C(R_1 + R_{ext})} - \frac{R_1 + R_2 + R_{ext}}{R_2 C(R_1 + R_{ext})} U_c(t) \quad (1)$$

where $U_c(t)$ is the voltage at the internal capacitor, R_{ext} is the external resistance, U_{oc} is the apparent open circuit voltage.

By applying Kirchoff's circuit law to the diagram in Fig. 2, the following analytical solution can be used to obtain MFC output voltage (U_{MFC}) as a function of time at low operating frequencies:

$$U_{MFC}(t) = U_{oc} - U_c(t) \frac{R_{ext}}{(R_1 + R_{ext})} \quad (2)$$

where

$$U_c(t) = U_{final} + U_{c,t0} - U_{final} e^{-t/\tau} \quad (3)$$

Here, the capacitance final voltage U_{final} and the time constant τ are defined as:

$$U_{final} = U_{oc} \frac{R_2}{R_1 + R_2 + R_{ext}}, \tau = \frac{R_2(R_1 + R_{ext})}{R_1 + R_2 + R_{ext}} C \quad (4)$$

At high frequencies of R_{ext} connection/disconnection, the voltage over the capacitance is considered to be a constant equal to the value of U_{final} . It can be expressed as a function of duty cycle ($D = t/T$) according to the following equation :

$$U_c = \frac{DR_2}{R_1 + R_{ext} + DR_2} U_{oc} \quad (5)$$

Then $U_{MFC}(t)$ can be calculated as

$$U_{MFC}(t) = U_{oc} - U_c - IR_1 \quad (6)$$

The analytical solution described above can be used for real-time estimation of key process parameters, such as R_1 , R_2 , C , and U_{oc} . In the proposed procedure, R_1 is estimated during MFC operation at high frequency (e.g. equal or above 100 Hz). Under these conditions U_c is assumed to be constant and can be estimated when the MFC is in the open-circuit mode (R_{ext} not connected). Then R_2 and C are estimated when the MFC is operated at a low frequency (e.g. below 1 Hz).

In more details, at high operating frequencies U_{MFC} is assumed to be at either high (U_{high}) or low (U_{low}) levels. With respect to ECM model in Fig. 2 and Eq. (5), the two voltage levels are related as follows:

$$U_{low} = U_{high} \frac{DR_2}{R_1 + R_{ext} + DR_2} \quad (7)$$

Notably, U_{low} and U_{high} are measurable values, and R_{ext} is known. Hence Eq. (7) can be used for R_1 estimation.

Subsequently, U_{oc} estimation can be obtained by MFC operating at a sufficiently low frequency. In this case, U_{oc} can be assumed equal to the voltage at the end of the “open-circuit” part of the cycle.

Furthermore, R_2 and C estimations can be also obtained using voltage measurements at low operating frequencies. Here, R_2 can be obtained with respect to Eq. (5) as

$$U_{final} = U_{oc} \frac{DR_2}{R_1 + R_{ext} + DR_2} \quad (8)$$

where U_{final} corresponds to MFC voltage at the end of the close-circuit part of the low frequency cycle.

To demonstrate on-line parameter estimation and compare the on-line and off-line estimations (obtained at the end of each experimental phase), we operated MFC at several influent flow rates of the concentrated stock acetate solution. The resulting profile of acetate flow rate is shown in Fig. 3.

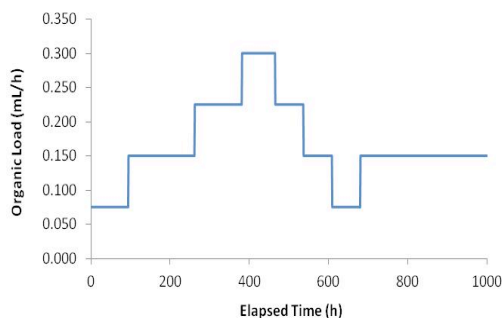


Fig. 3. Flow rates of acetate stock solution.

Fig. 4 compares R_1 estimations obtained following the on-line estimation procedure described above with the results of the off-line parameter estimation. With an exception of a short period following MFC operation at low organic load (around $t=700$ h), there was a good agreement between the two estimation methods. Interestingly, there was no immediate effect of influent acetate concentration (organic load) on the estimated R_1 value. However, MFC operation with progressively increasing organic loads between $t=100$ h and $t=500$ h led to lower R_1 values. Sharp decreases were observed at around $t = 180$ h and then around $t=300$ h (Fig. 4). Shortly after the start-up of MFC operation at low organic load (around $t= 600$ h), the off-line identification procedure indicated R_1 increase, while the on-line estimation showed no significant impact (Fig. 4). Both methods detected R_1 increase at around $t = 850$ h, which was not directly associated with a change in influent carbon source concentration.

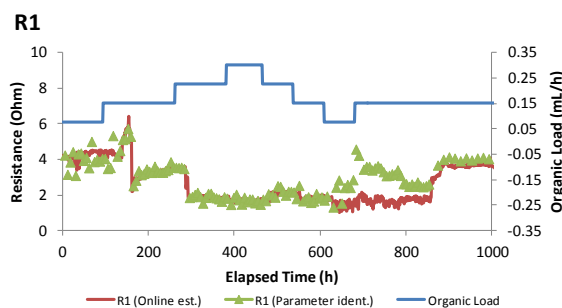


Fig. 4. Results of on-line and off-line estimation of R_1 .

Analysis of R_2 estimations shown in Fig. 5 suggested a strong link of this parameter with acetate availability in the anodic liquid. Progressive increase of the organic load starting from $t = 100$ h (Fig. 3) resulted in lower values of R_2 and this trend was confirmed both by on-line and off-line estimations. Similarly, organic load decrease at around $t = 600$ h led to almost immediate increase in R_2 . Interestingly, R_2 is often associated with activation losses at the anode (Yang et al. 2012). High activation losses might be expected at low acetate concentrations (low organic loads) due to carbon source - limited metabolism of anodophilic microorganisms.

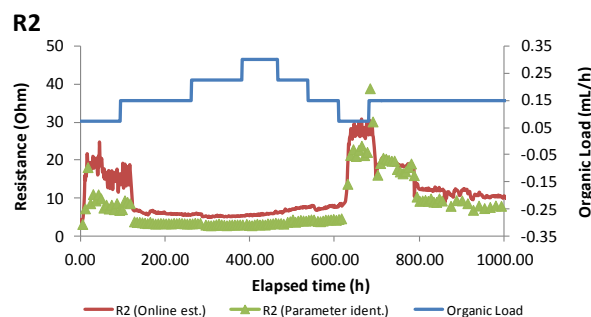


Fig. 5. Results of on-line and off-line estimation of R_2 .

Furthermore, a comparison of model-based internal resistance estimations calculated as $R_{int}=R_1 + R_2$ with experimental results obtained in polarization tests is shown in Fig. 6. This comparison clearly confirmed the acceptable accuracy of on-line estimations.

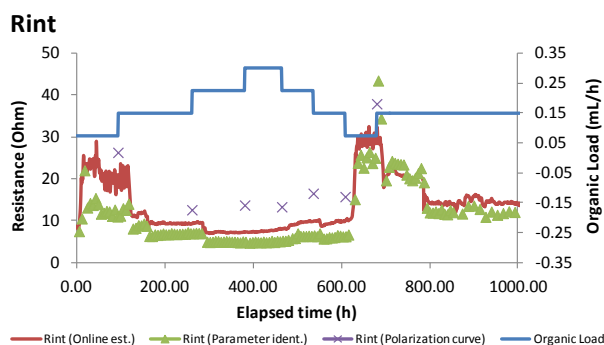


Fig. 6. Comparison of R_{int} estimations (on-line and off-line) with experimentally measured values based on polarization tests.

In addition to R_{int} estimations, the parameter estimation procedure demonstrated carbon source – related changed in V_{oc} , as shown in Fig. 7. In this case, the off-line estimation procedure appeared to provide a somewhat better response to variations in acetate load, e.g. at $t=100h$ (load increase) and $t = 600$ (load decrease). Nevertheless, when compared with the results of polarization tests, both estimations appeared to be significantly lower than the V_{oc} values measured in the experiment with a 30 min disconnection (open circuit) period. It should be taken into consideration, however, that relatively long periods (dozens of minutes) of MFC operation with a disconnected external resistance might lead to carbon source accumulation in the anodic liquid, which in turn is expected to alter the measurements.

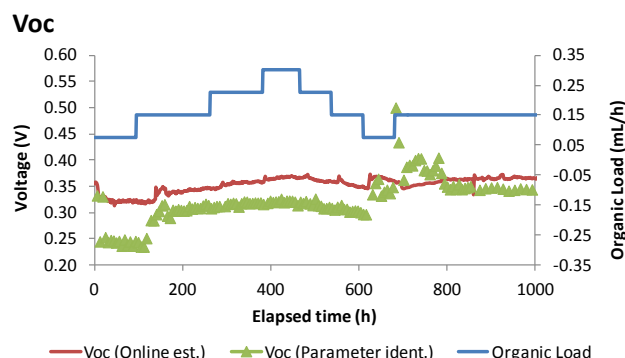


Fig. 7. Results of on-line and off-line estimation of U_{oc} .

Overall, D-tests suggested an increase in power output as a result of MFC operation in R-PWM mode. To elaborate on

this observation, two MFCs were operated for 3-5 days in the R-PWM mode with 95% duty cycle and external resistance values chosen based on R_{int} estimations obtained in the polarization tests. Then the operating mode was changed to constant connection and the MFCs were operated for another 3-5 days. To ensure optimal performance during this period, R_{ext} value was optimized in real time using the P/O algorithm described in Grondin et al. (2012). This sequence of testing was repeated several times. Interestingly, similar currents (and therefore similar Coulombic efficiencies) were observed, while both MFC voltages and power outputs were consistently higher during R-PWM tests. Since at an influent acetate concentration of 900 mg L⁻¹ the anodic liquid measurements showed acetate – limiting conditions with acetate levels below 40 mg L⁻¹, the tests were repeated where the influent concentration of acetate was doubled (1800 mg L⁻¹). The increased acetate load led to higher acetate concentrations in the anodic liquid (600-700 mg L⁻¹) and somewhat lower Coulombic efficiency. Nevertheless, the results once again confirmed improved power output during R-PWM operation.

Power outputs obtained during each MFC operation by the P/O algorithm were used as a basis for comparison (control) with the R-PWM mode of operation. The results of this comparison are summarized in Table 1 (current and power outputs were estimated based on the last 24 h of operation).

Table 1. A comparison of average currents, power outputs and Coulombic Efficiencies (CE) obtained during R_{ext} - PWM and Perturbation/Observation tests carried out at two influent acetate concentrations.

Influent acetate mg L ⁻¹	Cell	R-PWM mode			Perturbation/Observation		
		current mA	Power mW	CE %	current mA	Power mW	CE %
900	MFC-1	16.4	3.63	91.5	14.4	2.83	80.3
900	MFC-2	13.6	3.62	76.1	14.1	2.55	78.6
1800	MFC-1	15.1	3.84	42.2	17.1	3.07	47.9
1800	MFC-2	20.6	3.60	57.6	19.6	3.46	54.9

Power outputs observed during R-PWM tests were in a range of 3.6 – 3.8 mW corresponding to a volumetric power density of 72-76 mW L⁻¹. This power density is not only higher than that observed during MFC operation using the P/O algorithm (2.6 – 3.5 mW or 51-70 mW L⁻¹, Table 1), but also is higher in comparison to the recently reported performance of a continuously operated MFC with a power density of 30-50 mW L⁻¹ (Ahn & Logan, 2012).

Finally, the evolution in time of parameter C was also studied, as shown in Figure 8. In this case, it was the online parameter identification routine which proved a higher variability. As it could be expected, both estimation methods showed that capacitance increases as microbial activity does. As a fact, as more bacteria grow inside the bioreactor, the greater its capacity to storage energy, what validates once again the capacitance C as a parameter that allows the follow-up of microbial activity for a process control purpose.

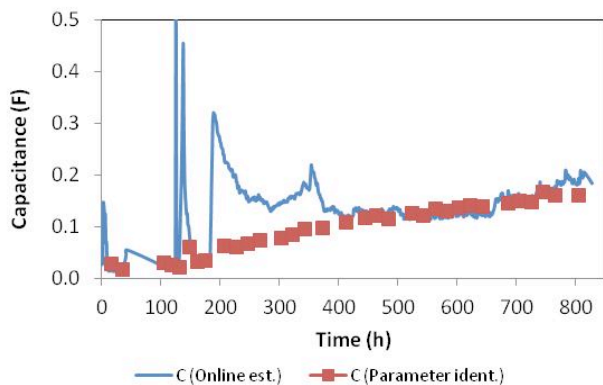


Figure 8 Evolution of capacitance estimation over time.

Interestingly, the periodic and pulse modes of operation of catalytic reactors were observed to lead to an increased catalyst activity and therefore an increased volumetric performance (Roopsing and Chidambaram, 1999). Several mechanisms were proposed to explain the increased catalyst activity, including a change in the catalyst state in response to reactant concentration, a higher catalyst activity due to a transient state, and non-linear reaction kinetics. While a direct comparison between the periodic operation of chemical reactors and the R-PWM mode of MFC operation might not be always justified, both systems feature catalysts with non-linear reaction kinetics. It can be suggested that at high-frequencies the R-PWM mode of MFC operation leads to a reduced activation and/or concentration losses due to changes in the biocatalytic activity. These losses are represented as R_2 in the equivalent circuit model. Also, it can be suggested that the carbon source concentration increases when R_{ext} is disconnected due to decreased consumption. This higher carbon source concentration positively affects the metabolic activity of the anodophilic microorganisms when R_{ext} is reconnected. Indeed, the anodophilic microorganisms were shown to exhibit a non-linear (Monod or Haldane-like) kinetics of carbon source consumption. These hypotheses might require extensive validation using experimental methods and through model-based analysis.

4. CONCLUSIONS

This study demonstrates that MFC operation with pulse-width modulated connection of the external resistor (R-PWM mode) enables on-line monitoring and parameter estimation of key MFC parameters, such as internal resistance and open circuit voltage. The on-line parameter estimation procedure might be instrumental in developing robust MFC-based wastewater treatment systems capable of operating under a broad range of operating conditions and handling various organic loads.

REFERENCES

- Ahn, Y., & Logan, B. (2012). A multi-electrode continuous flow microbial fuel cell with separator electrode assembly design. *Appl Microbiol Biotechnol* 93, 2241-2248.
- Durr M., Cruden A., Gair S., McDonald J.R. (2006). Dynamic model of a lead acid battery for use in a domestic fuel cell system. *J. Power Sources* 161:1400-1411.
- Grondin F., Perrier M., Tartakovsky B. (2012). Microbial fuel cell operation with intermittent connection of the electrical load. *J. Power Sources* 208:18-23.
- Logan B. (2010). Scaling up microbial fuel cells and other bioelectrochemical systems. *Appl. Microbiol. Biotechnol.* 85:1665-1671.
- Logan B., Rabaey K. (2012). Conversion of Wastes into Bioelectricity and Chemicals by Using Microbial Electrochemical Technologies. *Science* 337:686-690.
- Lovley D.R. (2008). The microbe electric: conversion of organic matter to electricity. *Current Opinion Biotechnol.* 19:564-571.
- Martin E., Savadogo O., Guiot S.R., Tartakovsky B. (2010). The influence of operational conditions on the performance of a microbial fuel cell seeded with mesophilic sludge. *Biochem. Eng. J.* 51:132-139.
- Park J.-D., Ren Z. 2011. Efficient Energy Harvester for Microbial Fuel Cells. *Energy Conversion Congress and Exposition (ECCE), IEEE.* Phoenix, AZ, USA. p 3852 - 3858.
- Pinto R.P., Srinivasan B., Guiot S.R., Tartakovsky B. (2011). The Effect of Real-Time External Resistance Optimization on Microbial Fuel Cell Performance. *Wat. Res.* 45:1571-1578.
- Premier G.C., Kim J.R., Michie I., Dinsdale R.M., Guwy A.J. (2011). Automatic control of load increases power and efficiency in a microbial fuel cell. *J. Power Sources* 196 2013-2019.
- Roopsingh, G. M. Chidambaram, *Bioprocess Eng.* 20 (1999) 279-282.
- Rozendal R.A., Hamelers H.V.M., Rabaey K., Keller J., Buisman C.J.N. (2008). Towards practical implementation of bioelectrochemical wastewater treatment. *Trends in Biotechnol.* 26:450-459.
- Yang F., Zhang D., Shimotori T., Wang K.-C., Huang Y. (2012). Study of transformer-based power management system and its performance optimization for microbial fuel cells. *Journal of Power Sources* 205:86-92.